A Study on the Dip-pen Nanolithography Process and Fabrication of Optical Waveguide for the Application of Biosensor

Jun-Hyong Kim and Hoe-Young Yang
Interdisciplinary Program of Photonic Engineering, Chonnam Natioanl University, 300 Yongbong-dong, Buk-gu, Gwangju 500-757, Korea

Chong-Hee Yu
Optical Communications Research Center, Electronics and Telecommunications Research Institute, 1110-6 Oryong-dong, Buk-gu, Gwangju 500-480, Korea

Hyun-Yong Lee[a]
Center for Functional Nano Fine Chemicals, Faculty of Applied Chemical Engineering, Chonnam National University, 300 Yongbong-dong, Buk-gu, Gwangju 500-757, Korea

[a]E-mail : hyleee@chonnam.ac.kr

(Received January 4 2008, Accepted July 3 2008)

Photonic crystal structures have been received considerable attention due to their high optical sensitivity. One of the techniques to construct their structure is the dip-pen lithography (DPN) process, which requires a nano-scale resolution and high reliability. In this paper, we propose a two dimensional photonic crystal array to improve the sensitivity of optical biosensor and DPN process to realize it. As a result of DPN patterning test, we have observed that the diffusion coefficient of the mercaptohexadecanoic acid (MHA) molecule ink in octanol is much larger than that in acetonitrile. In addition, we have designed and fabricated optical waveguides based on the mach-zehnder interferometer (MZI) for application to biosensors. The waveguides were optimized at a wavelength of 1550 nm and fabricated according to the design rule of 0.45 delta%, which is the difference of refractive index between the core and clad. The MZI optical waveguides were measured of the optical characteristics for the application of biosensor.

Keywords : Dip-pen nanolithography, Mach-zehnder interferometer, Photonic crystal, Optical biosensor

1. INTRODUCTION

Applications to biosensors tend to be made in a more miniaturized and systemized fashion. Much research has investigated the development of a small site, high sensitivity and low cost biosensor using semiconductor integration and nano technique, which enable the detection of a very limited amount of samples. Commercial biosensors, e.g., surface-plasmon resonance (SPR) sensors[1], detect selective binding by measuring the refractive index change on the sensing arm.

However, this method requires a relatively high sensitive range (~1 mm^2) in terms of the condition of the exact direction or angle. The evanescent-wave sensor based on the mach-zehnder interferometer (MZI) principle has sufficiently high sensitivity to measure the change of the refractive index on the surface of a waveguide[2-5]. This is because the sensor is suitable for directly recognizing an antigen that reacts to the molecule of an antibody receptor adhered to the surface of a waveguide.

Sensor applications using photonic crystals[5-7] are attracting research attention because photonic crystals have a photonic bandgap with a wide range of frequency and they create a defect that can perform resonance for the light of an intentionally internal single frequency. Sensing is performed by measuring the wavelength shift of the photonic band edge due to the change of refractive-index distortion inside and around the photonic crystal caused by the introduction or the

adsorption of material. Since the change of transmittance at the photonic band edge is extremely sharp, a high sensitivity is expected. In particular, a very small micro-cavity with a high quality factor (Q) has a very small sensing area (~1 μm^2) and needs a very small amount of sample to be measured. That is, photonic crystals are very appropriate to the application of a biosensor. In addition, it is possible to integrate many functions on a chip. However, a reliable, nano-scale lithography process with high resolution is required to realize the photonic crystal structures necessary to increase the sensor sensitivity. So far, existing photonic crystals have been implemented mainly through electron-beam lithography[8-10] and x-ray lithography[11]. However, these methods suffer a resolution limitation, and are accompanied by complex processes because they include photo-resist development and substrate etching processes [8-15]. Therefore, it seems that a new and reliable, process technique should be developed for the next generation photonic crystal technique. It is important to secure a fabrication technique capable of fabricating a nano-sized pattern and growing the desired photonic crystals directly on a substrate without resist process.

Dip-pen nanolithography (DPN)[16-22] developed in 1999 is the nano patterning technique that coats molecules in an atomic force microscope (AFM) tip and imprints the molecules to a substrate.

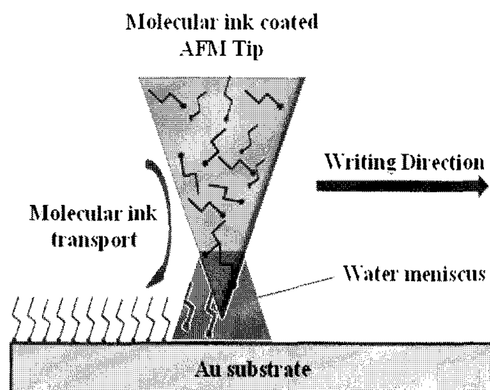

Fig. 1. Schematic diagram of the dip-pen nanolithography.

DPN, as shown in Fig. 1, used an AFM tip as a "nib", a solid-state substrate as "paper" and molecules with a chemical affinity for the solid-state substrate as "ink" [16]. The principle of the DPN is to transport the patterning materials from the AFM tip the solid-state substrate because the humidity in the air would form a water meniscus between them while the tip contacts with the substrate.

DPN is a new nano-patterning technique with a maximum resolution of 15 nm.

In this paper, we present several experiment data for the DPN process to implement photonic crystal array on the sensor arm. In addition, we propose the design of MZI-type optical waveguides for an optical biosensor and discuss their characteristics.

2. EXPERIMENT

2.1 Process of dip-pen nanolithography

DPN patterning process and image measurement were performed by using the CP-II AFM and micro cantilever tip (sharpened Microlever A, force constant = 0.05 N/m, Si_3N_4).

All of the tips were then coated with the alkanethiol mercaptohexadecanoic acid (MHA) by dipping into a solution of MHA in acetonitrile or octanol. The cleaned tips were placed in freshly prepared MHA solution for 10 s, and then blown dry N_2. The substrate was prepared by sputtering a layer of 25 nm Au on top of a (100) silicon wafer with a Ti adhesion layer of 5 nm. To wash the Au substrate, the first-step washing to remove organic matters and the second-step washing to remove the remnant are performed. For the first-step washing, the Au substrate is dipped into boiling acetone for a minute and ultrasonic washing is performed for the substrate in isopropyl alcohol (IPA) for a minute. After the procedures, the substrate is washed out in distilled water. For the second-step washing, the Au substrate is washed in the NH_4OH : H_2O_2 (1 : 1) solution at 75 ~ 85 °C for a minute and washed out in distilled water. After the procedures, the substrate is dried in N_2 gas.

The DPN process was performed in a glove box that can control humidity and temperature to 38 ~ 40 % and 24 ~ 26 °C, respectively.

The scan rate of the tip during DPN patterning process was set to 1 Hz. To compare the diffusion coefficients when MHA ink with a different solvent was used, the contact time between the tip and the substrate during the DPN patterning was set to 4, 6, 10, and 15 s. After patterning, MHA dots were immediately imaged with the same tip in lateral force microscopy (LFM) imaging mode. The pattern was read by the same tip with high scan rate (4 Hz) to avoid depositing MHA ink over entire area during obtaining images.

2.2 Design and fabrication of MZI waveguides

The design and fabrication conditions used to prepare the symmetric and asymmetric MZI waveguides for application to the biosensors are summarized in Table 1. The waveguide was optimized at a wavelength of 1550 nm and the difference of the refractive index between core and clad was 0.45 delta%.

Table 1. Design and fabrication condition of symmetric and asymmetric optical waveguide.

Parameter	Symmetric	Asymmetric
Input light source (nm)	1550	1550
Core (n_{core})	~1.451	~1.451
Clad (n_{clad})	~1.444	~1.444
Core size (μm^2)	6	6
Sensor arm length (μm)	1200	1000
Sensor length (mm)	10	17.5

The fabrication of symmetric and asymmetric MZI optical waveguides was performed by a conventional planar lightwave circuit (PLC) fabrication process and DPN process. The fabrication procedure is shown in Fig. 2.

The schematic structures of the MZI sensor fabricated for application to the biosensors are shown in Fig. 3, where (a) and (b) indicate the symmetric and asymmetric MZI optical waveguide structure and result of simulated light strength depending on the location of light penetration when light is transmitted to the input block of a waveguide, respectively.

An input signal is branched into two parts through the first Y-branch waveguide, and each part passes through the reference path of interferometer and the path for sensing. Subsequently, they are combined in the second Y-branch and exit through the output waveguide.

The MZI waveguide consists of under-clad, core and over-clad, as for a general integrated optical device. For one path of the interferometer, the over-clad is removed and then the part contacts with a cover layer. If the refractive index of the sensing arm cover layer is changed, the phase of the light transmitted through this path differs from that of the light transmitted through another path reference part. Thus, the two paths which transmit through each other are interfered at the output port. The output intensity generally follows the relationship of $I \propto [1+V\cos\Delta\Phi]$, and the phase difference between the two paths, $\Delta\Phi$, is represented by $\Delta\Phi=2\pi L\Delta N\text{clad}/\lambda$.

Here, λ is the wavelength of the light, ΔN the change of effective refractive index according to the cover layer material, and L the length of the sensing arm. Thus, measuring the light intensity through MZI strongly depends on the change of the effective refractive index according to the cover layer material. The pulses shown in Fig. 3 represent the field distribution in several ports on the MZI waveguides.

An auto alignment system is used to measure the characteristics of the fabricated symmetric and asymmetric MZI optical waveguide devices. To evaluate the insertion loss (IL) and polarization dependent loss (PDL), the interface of the PLC device and optical fiber was pasted by index matching oil.

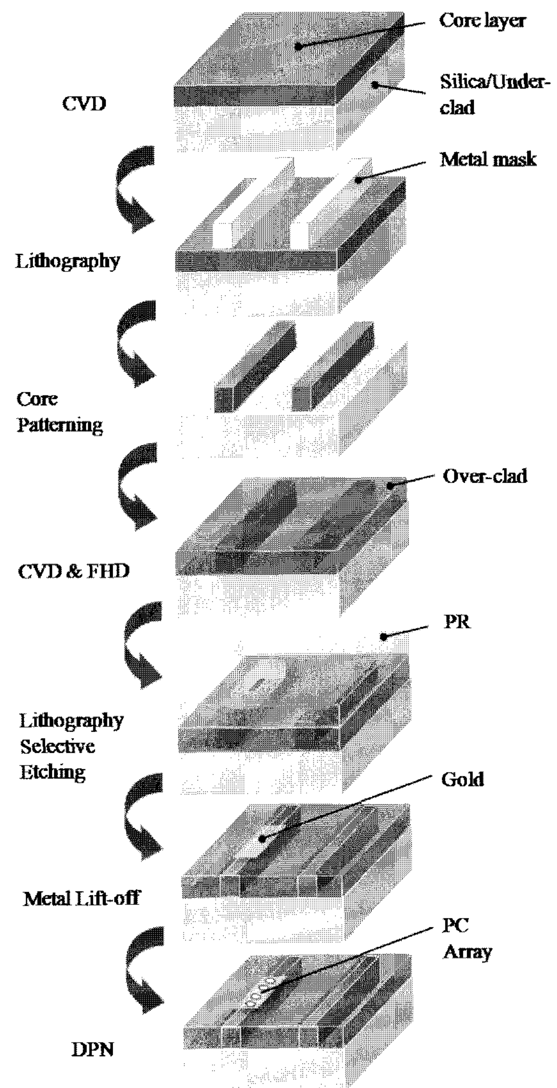

Fig. 2. Fabrication procedures of symmetric and asymmetric MZI optical waveguides containing PLC and DPN processes. Silica planar waveguides are patterned by photolithography process. Channel waveguide for PLCs are etched by using reactive ion etching and inductively coupled plasma etching. Patterned cores are covered with thick SiO_2 claddings (over-cladding) using chemical vapor deposition (CVD) or frame hydrolysis deposition (FHD) method to bury the waveguides for high efficiency and safekeeping.

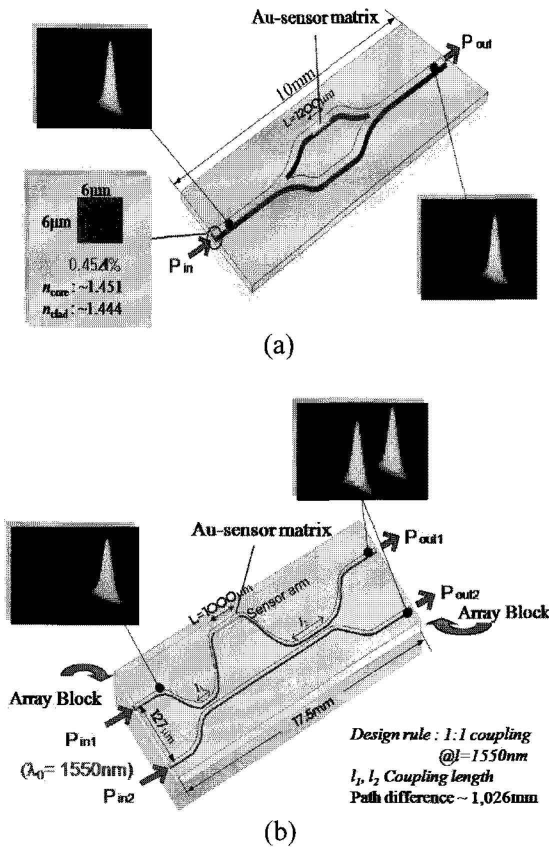

Fig. 3. Schematic diagrams of an MZI sensor fabricated for application to the biosensors. (a) Symmetric MZI optical waveguide structure, and (b) asymmetric MZI optical waveguide structure.

3. RESULTS AND DISCUSSION

The diffusion coefficient of the molecule ink was measured for its reproducibility and the pattern with the desired size through the DPN patterning process. The dot area after the DPN patterning can be calculated according to the following relationship:

$$A = \pi \cdot r^2 = C \cdot \Delta t$$

where A, r, C and Δt are the area, radius, diffusion coefficient and dwell time, respectively.

Figure 4 shows the result of the DPN patterning test performed by using the MHA molecule inks. Figs. 4(a) and 4(b) indicates the LFM image of the dot pattern by using the MHA in acetonitrile and octanol respectively. The LFM image showing the pattern based on measurements as the contact time between the tip and substrate increased (4, 6, 10, and 15 seconds). Fig. 4(c) indicates the relation between the dot area and the dwell time based on the measurement result.

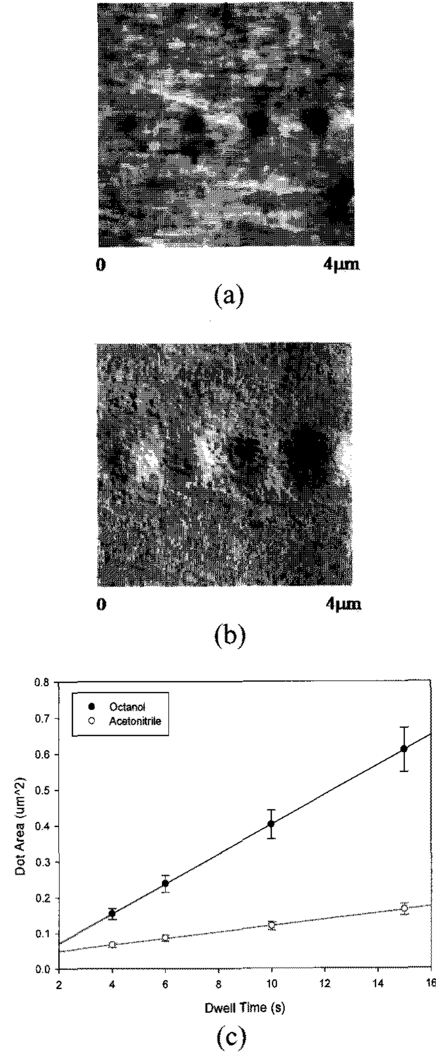

Fig. 4. Result of the DPN patterning performed by using the MHA molecule ink with a different solvent. (a) Lateral force microscopy image of dots patterned using the MHA molecule ink with acetonitirle at the solvent. (b) Lateral force microscopy image of dots patterned using the MHA molecule ink with octanol as the solvent. (c) Plot of relationship between the dot area and dwell time.

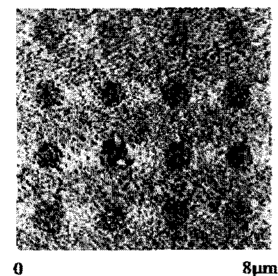

Fig. 5. Result of the DPN patterning test for 4 × 4 MHA dot by using the MHA molecule ink in octanol.

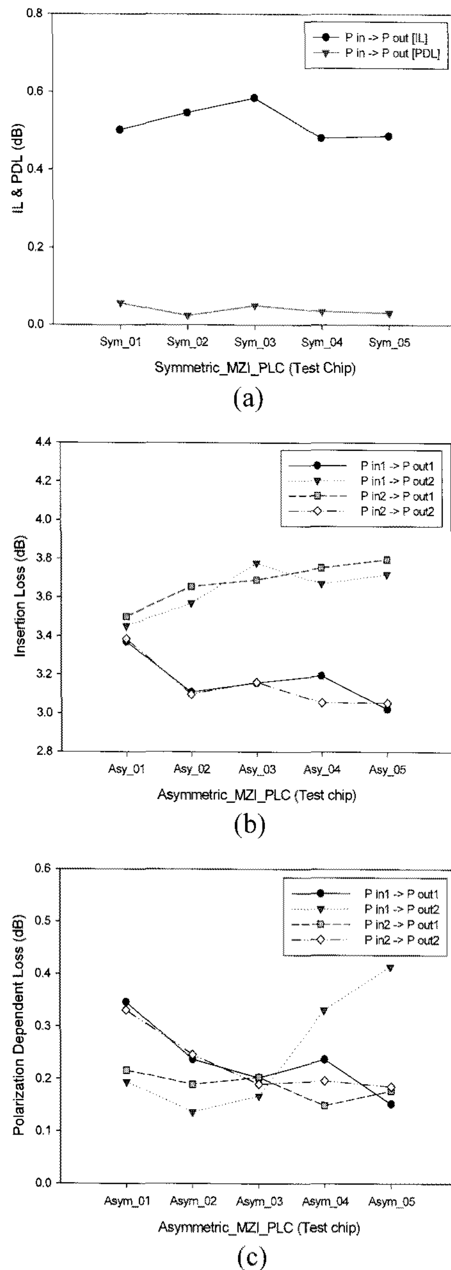

Fig. 6. Optical characteristics of symmetric and asymmetric MZI optical waveguides devices measured at a wavelength of 1550 nm. (a) Insertion loss and polarization dependent loss of symmetric MZI optical waveguide. (b) Insertion loss of asymmetric MZI optical waveguide. (c) Polarization dependent loss of asymmetric MZI optical waveguide.

According to the LFM measurement result, the dot pattern of MHA molecules was formed on the Au surface. The diffusion coefficients of the MHA molecule ink in acetonitrile and octanol was 0.0895956 $\mu m^2/s$ and 0.04139023 $\mu m^2/s$ respectively. According to the analysis indicating that the diffusion coefficient of the MHA molecule ink in octanol is much larger than that in acetonitrile. Thus, if octanol is used as the solvent of the MHA molecule ink, many patterns can be created more efficiently and rapidly.

Figure 5 shows the result of the DPN patterning test for the 4 × 4 MHA dot using the MHA molecule ink in octanol, in which the formation of a dot pattern with the same size is evident.

The fabricated MZI optical waveguide device was measured while the sensor was not etched. The results appear in Fig. 6. According to the measurement result, the insertion loss of symmetric MZI optical waveguide device was below 1 dB and the PDL was within 0.1 dB. For the asymmetric MZI optical waveguide device, the branch rate was about 3 dB when each channel of the input and output ports was measured.

In future research, the Au thin film will be deposited in the sensor ports of an existing MZI optical waveguide device and the optical characteristics that depend on the thickness of the thin film will be compared and evaluated. In addition, the optimized condition for the DPN process will be secured to fabricate a two-dimensional photonic crystal structure.

4. CONCLUSION

This research has proposed the DPN process that presented to implement the two-dimensional photonic crystal structure with the benefit of greatly enhancing the sensor sensitivity. By using octanol as the solvent of the MHA molecule ink, which is used during the DPN patterning test, it was evident that many patterns were created more efficiently and rapidly. However, to establish the optimized process condition for the fabrication of a stabilized pattern, many preliminary tests under various process conditions are required. We therefore consider that if the optimized DPN process condition is secured in the future, it will be possible to fabricate a reliable two-dimensional photonic crystal arrangement with high resolution.

In addition, we have fabricated the symmetric and asymmetric MZI optical waveguides for application to the biosensors. As a result, we were able to obtain that optical characteristic of MZI waveguide devices was low insertion loss and low PDL. It is therefore possible to apply these facts to be optical-biosensors. For the fabrication of an optical biosensor with an integrated MZI configuration, the optical waveguides must have a high surface sensitivity.

ACKNOWLEDGMENTS

This work was supported by Grant No. RTI04-03-03 from the Regional Technology Innovation Program of

the Ministry of Knowledge Economy(MKE). This work was supported by the Korea Research Foundation Grant funded by the Korean Government(MOEHRD) (KRF-2007-412-J02003).

REFERENCES

[1] J. Homola, S. S. Yee, D. Myszka, in: F. S. Ligler, C. A. Rowe Taitt (Eds.), "Optical Biosensors", Elsevier, Amsterdam, p. 207, 2002.

[2] E. F. Schipper, A. M. Brugman, C. Domingues, L. M. Lechuga, R. P. H. Kooyman, and J. Greve, "The realization of an integrated Mach-Zehnder waveguide immunosensor in silicon technology", Sens. Actuators, B 40, p. 147, 1997.

[3] F. Prieto, B. Sepulveda, A. Calle, A. Llobera, C. Dominguez, and L. M. Lechuga, "Integrated Mach-Zehnder interferometer based on ARROW structures for biosensor applications", Sens. Actuators, B 92, p. 151, 2003.

[4] A. K. Sheridan, R. D. Harris, P. N. Bartlett, and J. S. Wilkinson, "Phase interrogation of an integrated optical SPR sensor", Sens. Actuators, B 97, p. 114, 2004.

[5] R. Levy, A. Peled, and S. Ruschin, "Waveguided SPR sensor using a Mach-Zehnder interferometer with variable ratio", Sens. Actuators, B 119, p. 20 2006.

[6] E. Yablonovitch, "Photonic band-gap structures", J. Opt. Soc. Am., B 10, No. 2, p. 283, 1993.

[7] E. Yablonovitch, "Photonic crystals", J. Mod. Opt., Vol. 41, No. 2, p. 173, 1994.

[8] J. D. Joannopoulos, R. D. Meade, and J. Winn, "Photonic Crystals", Princeton Univ. Press, Princeton, 1995.

[9] J. Fujita, Y. Ohnishi, Y. Ochiai, and S. Matsui, "Ultrahigh resolution of calixarene negative resist in electron beam lithography", Appl. Phys. Lett., Vol. 68, No. 9, p. 1297, 1996.

[10] J. M. Gibson, "Reading and writing with electron beams", Phys. Today, Vol. 50, No. 10, p. 56, 1997.

[11] S. B. Clendenning, S. Aouba, M. S. Rayat, D. Grozea, J. B. Sorge, P. M. Brodersen, R. N. S. Sodhi, Z. H. Lu, C. M. Yip, M. R. Freeman, H. E. Ruda, and I. Manners, "Direct writing of patterned ceramics using electron-beam lithography and metallopolymer resists", Adv. Mater., Vol. 16, No. 3, p. 215, 2004.

[12] W. Chu, H. I. Smith, and M. L. Schattenburg, "Replication of 50 nm linewidth device patterns using proximity x-ray lithography at large gaps", Appl. Phys. Lett., Vol. 59, No. 13, p. 1641, 1991.

[13] J. G. Goodberlet, "Patterning 100 nm features using deep-ultraviolet contact photolithography", Appl. Phys. Lett., Vol. 76, No. 6, p. 667, 2000.

[14] P. J. Silverman, "The interl lithography roadmap", Intel Technol. J., Vol. 6, No. 2, p. 55, 2002.

[15] H. S. Kim, D. H. Shin, S. K. Kim, J. K. Rhee, B. S. Lee, H. W. Kim, J. U. Lee, Y. S. Han, and Y. H. Choe, "Fabrication technology for improving pattern quality in two-dimensional photonic crystal structure", J. of KIEEME(in Korean), Vol. 16, No. 6, p. 515, 2003.

[16] R. D. Piner, J. Zhu, F. Xu, S. Hong, and C. A. Mirkin, "Dip-pen nanolithography", Science, Vol. 283, p. 661, 1999.

[17] R. D. Piner, S. Hong, and C. A. Mirkin, "Improved imaging of soft materials with modified AFM tips", Langmuir, Vol. 15, No. 17, p. 5457, 1999.

[18] S. Hong, J. Jhu, and C. A. Mirkin, "A new tool for studying the in situ growth processes for self-assembled monolayers under ambient conditions", Langmuir, Vol. 15, No. 23, p. 7897, 1999.

[19] S. H. Hong, J. Zhu, and C. A. Mirkin, "Dip-pen nanolithography", Science, Vol. 286, p. 523, 1999.

[20] D. A. Weinberger, S. G. Hong, B. W. Wessels, and T. B. Higgins, "Combinatorial generation and analysis of nanometer- and micrometer-scale silicon features via 'Dip-pen' nanolithography and wet chemical etching", Adv. Mater., Vol. 12, No. 21, p. 1600, 2000.

[21] B. W. Maynor, Y. Li, and J. Liu, "Au 'Ink' for AFM 'Dip-pen' nanolithography", Langmuir, Vol. 17, No. 9, p. 2575, 2001.

[22] J. Haaheim, R. Eby, M. Nelson, J. Fragala, B. Rosner, H. Zhang, and G. Athas, "Dip-pen nanolithography (DPN): process and instrument performance with Nanoink's NSCRIPTOR system", Ultramicroscopy, Vol. 103, No. 2, p. 117, 2005.